

One-nucleon stripping reactions to discrete levels induced by a 480 MeV ^{12}C beam on a ^{208}Pb target

M. C. Mermaz, E. Tomasi-Gustafsson, B. Berthier, R. Lucas, J. Gastebois,
A. Gillibert, and A. Miczaika

*Département de Physique Nucléaire, Centre d'Etude Nucléaire de Saclay,
91191 Gif-sur-Yvette Cedex, France*

A. Boucenna, L. Kraus, I. Linck, B. Lott, R. Rebmeister, N. Schulz, and J. C. Sens
Centre de Recherche Nucléaire et Université Louis Pasteur, 67037 Strasbourg, Cedex, France

C. Grunberg

Grand Accélérateur National d'Ions Lourds, Caen, 14021 Caen Cedex, France

(Received 21 October 1987)

One-proton and one-neutron stripping reactions induced by a 480 MeV ^{12}C beam bombarding a ^{208}Pb target have been studied using a high resolution energy loss magnetic spectrometer. The reactions are governed by two selection rules which are naturally contained in the one-step exact finite range distorted wave Born approximation formalism. Relative intensities of the populated states are well reproduced by this formalism as well as the absolute values of the cross sections. Comparisons with the results of one-nucleon stripping reactions induced by a ^{16}O beam on a ^{208}Pb target at 793 MeV incident energy are also presented; in this latter case the absolute cross section values are not reproduced.

I. INTRODUCTION

One-nucleon transfer reactions have already been extensively studied experimentally and rather successfully compared with the exact finite range-distorted wave Born approximation (EFR-DWBA) predictions.¹⁻³ We shall present in this paper experimental data and theoretical analyses concerning very high incident energy: one-proton and one-neutron direct surface transfer reactions induced by a 480 MeV ^{12}C beam on a ^{208}Pb target. These present results will also be compared to our previous data obtained with a 793 MeV ^{16}O beam bombarding a ^{208}Pb target, and already partially published Refs. 4 and 5.

At high incident energy the values of the cross sections are governed by two selection rules contained in the EFR-DWBA and also in the semiclassical model of Brink.^{6,7} The first selection rule tells us that final states with high spin are strongly favored at high incident energy. This is due to the large mismatch between the entrance and exit grazing wave orbital angular momenta. The second selection rule tells us that the favored transition involves no spin-flip between the projectile wave function and the heavy residual nucleus wave function. We shall see that these two selection rules explain perfectly the relative intensities for the population of the single-particle states.^{4,5} However, we shall also see that the absolute values are well reproduced by the EFR-DWBA calculations in case of ^{12}C induced reactions, but definitively not in the case of ^{16}O induced reactions: a rather puzzling problem. A detailed study of the EFR-DWBA calculations at high incident energy will be presented, and, in addition, the transition to high spin

states at higher excitation energy will be tentatively analyzed.

II. EXPERIMENTAL ARRANGEMENT

The one-proton and one-neutron transfer reactions on a ^{208}Pb target were performed at the GANIL facility using the 480 MeV ^{12}C beam. The ejectile particles, ^{11}B and ^{11}C nuclei, were identified and momentum analyzed using the energy loss magnetic spectrometer SPEG (Ref. 8). The thickness of the ^{208}Pb target (99% enriched) was about 1.7 mg/cm² measured with the alpha gage techniques. The detection system consisted of (i) two position (x, y) drift chambers having a spatial resolution of 0.6 mm in each direction, located on each side of the focal surface in order to determine the scattering angle and the accurate magnetic rigidity of the detected particle, (ii) an ionization chamber which measured the energy loss of the outgoing particles, necessary for their identification, (iii) two plastic scintillators, the first one providing the start signal of the time of flight and the second one serving as a veto for the rejection of light particles. The rf of the last GANIL cyclotron provided the stop signal of the time of flight. All the gas counters were filled with isobutane. With this arrangement the measured energy resolution was about 200 keV full width at half maximum (FWHM), or translated into momentum resolution: $\Delta p/p \approx 2 \times 10^{-4}$. The total angular aperture of the spectrometer in the reaction plane was 4° and the counting rate normalization between runs was assured by a one degree overlap in angle. The beam emittance for all runs was never larger than 2π mm mrad which permits an an-

gular binning of 0.4° in the angular distributions. The absolute values for all cross sections were easily obtained due to the fact that the measured ^{12}C elastic cross section obeys the Rutherford law at forward angles.

III. RESULTS AND DISCUSSION

First, we shall present and discuss the results of the one-nucleon stripping reactions populating the low lying single particle states which have well-known spin assignments. Secondly, we shall present the results of the transfer data populating states at higher excitation energy for which high spin single particle configurations have been rather hypothetically assigned. Then finally, we shall present a general discussion concerning the EFR-DWBA predictions of cross section absolute values for one-nucleon stripping reactions.

A. One-nucleon stripping reactions populating the low lying single particle states

In Fig. 1 is presented the energy spectrum of the $^{208}\text{Pb}(^{12}\text{C}, ^{11}\text{B})^{209}\text{Bi}$ one-proton stripping reaction measured at 480 MeV ^{12}C incident energy along with the energy spectrum of the $^{208}\text{Pb}(^{16}\text{O}, ^{15}\text{N})^{209}\text{Bi}$ one-proton stripping reaction measured at 793 MeV ^{16}O incident en-

ergy.^{4,5} The relative intensities of the populations of the various single-particle states can be explained with the two selection rules previously discussed in the Introduction. For the $(^{12}\text{C}, ^{11}\text{B})$ reaction the strongest peak is the 1.608 MeV $1i_{13/2}^+$ favored by the two selection rules (i) high final angular momenta, $l=6$, and (ii) no spin flip transition: $l_f + \frac{1}{2}$, $(1i_{13/2}^+)$ final spin in ^{209}Bi residual nucleus for a $l_i + \frac{1}{2}(1p_{3/2}^3)$ initial spin in the projectile. On the other hand, for the $(^{16}\text{O}, ^{15}\text{N})$ reaction (initial state $1p_{3/2}^1$, $l_i - \frac{1}{2}$ in the projectile), the transition to the 1.608 MeV $1i_{13/2}^+$ which corresponds to a spin flip process is inhibited despite the large orbital angular momentum involved in the transfer process. For the $(^{16}\text{O}, ^{15}\text{N})$ reaction, the g.s. $1h_{9/2}^-$, $l=5$ transition is favored by the two selection rules and is thus the strongest peak for this stripping reaction, but in case of the $(^{12}\text{C}, ^{11}\text{B})$ reaction involving a spin flip transition, we observe a small peak for the g.s. yield: the transition is inhibited. Other interesting lines are the $2f_{7/2}^-$ and $2f_{5/2}^-$ states both $l=3$ transitions. It is then only the second selection rule concerning spin flip transitions which can explain the differences in intensities between these two levels in the $(^{12}\text{C}, ^{11}\text{B})$ and $(^{16}\text{O}, ^{15}\text{N})$ one proton stripping reactions. For the $(^{16}\text{O}, ^{15}\text{N})$ reaction, the no spin flip transition cor-

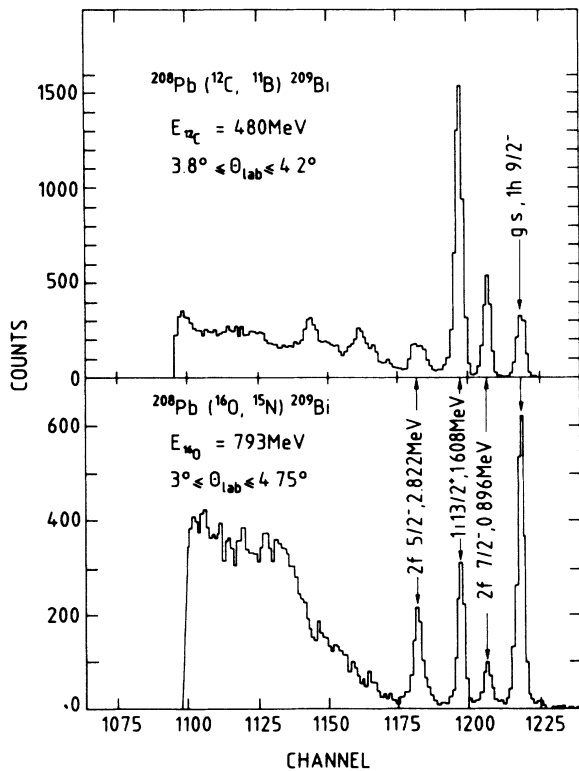


FIG. 1. Energy spectra for the one-proton stripping reactions induced by ^{16}O and ^{12}C beams at 793 and 480 MeV incident energies, respectively. Only high spin single-particle states are populated strongly. The energy resolution is about 200 keV FWHM.

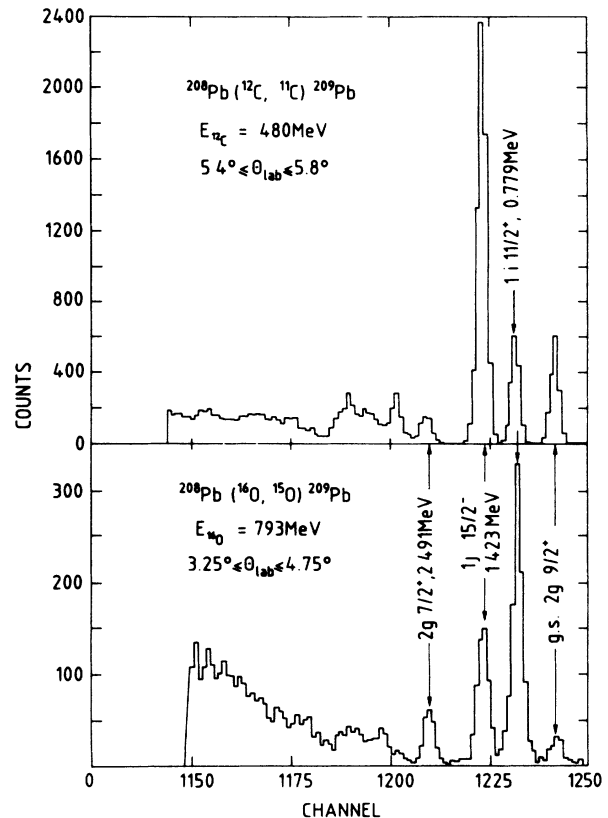


FIG. 2. Energy spectra for the one-neutron stripping reactions induced by ^{16}O and ^{12}C beams at 793 and 480 MeV incident energies, respectively. Only high spin single-particle states are populated strongly. The energy resolution is about 200 keV FWHM.

responds to the 2.822 MeV $2f_{7/2}^{-}$ state which has a stronger counting yield than the $2f_{5/2}^{-}$ level, see bottom of Fig. 1. On the other hand, the no spin flip transition for the ($^{12}\text{C}, ^{11}\text{B}$) reaction corresponds to the 0.896 MeV $2f_{7/2}^{-}$ state which has a stronger counting yield than the $2f_{5/2}^{-}$ level, see top of Fig. 1. For both one-proton stripping reactions let us note that the orbital angular momentum mismatch between the entrance and exit channel is $8\hbar$ for the grazing waves. This value of $8\hbar$ is obtained by inspection of the optical model S matrix elements of the entrance and exit channel: $S_{lg} = 0.50$. See later on, the elastic scattering and DWBA analysis. Other levels are populated in the ($^{12}\text{C}, ^{11}\text{B}$) reaction spectrum and will be discussed later on. In case of the ($^{16}\text{O}, ^{15}\text{N}$) reactions these additional lines are obscured by the excitation of the ejectile in its $1p_{3/2}^{-}$ single hole-state located at 6.324 MeV, see Refs. 4, 5, and 2.

In Fig. 2 are presented the one-neutron stripping reaction spectra induced by ^{12}C and ^{16}O projectile, respectively, on a ^{208}Pb target. The interpretation of these data follow the previous discussion. The strongest transitions for both reactions involve large angular momenta and no spin flip: they are the 1.423 MeV $1j_{7/2}^{-}$ level, $l=7$, for the ($^{12}\text{C}, ^{11}\text{C}$) reaction and the 0.779 MeV $1i_{11/2}^{+}$ level for the ($^{16}\text{O}, ^{15}\text{O}$) reaction.^{4,5} Let us note that the orbital angular momenta mismatch for the grazing waves is $10\hbar$ for both stripping reactions. The populations of the $2g_{7/2}^{+}$ and $2g_{5/2}^{+}$ states, both $l=4$, are governed in the two energy spectra only by the no spin flip selection rule; and their relative strengths are inverted in the two reactions. Other lines are also populated at higher excitation energy in the ($^{12}\text{C}, ^{11}\text{C}$) reaction and will be discussed later on. These lines are obscured in the ($^{16}\text{O}, ^{15}\text{O}$) reaction by the excitation of the ^{15}O ejectile on its $1p_{3/2}^{-}$ single hole state located at 6.176 MeV, see Refs. 4, 5, and 2.

In order to obtain absolute values for the stripping reaction cross sections and in order to perform a full EFR-DWBA calculation, the ^{12}C elastic scattering angular distribution has been measured. A Fresnel pattern is observed and has been analyzed in the framework of the optical model using in all our calculations a volume Woods-Saxon geometry for the real and imaginary part of the potential. A typical result of a best fit procedure is presented in Fig. 3. It was obtained with the code PTOLEMY (Ref. 9) which has no relativistic correction for elastic scattering and direct transfer reaction calculations. The family given in Fig. 3 corresponds to strong absorption and many other families can be deduced from the Igo ambiguity.¹⁰ This present family of Fig. 3 is alike to the one used to analyze the stripping reactions induced by the 793 MeV ^{16}O beam bombarding a ^{208}Pb target. It is worthwhile to note that this 50 MeV deep potential has its parameter values, in best agreement with the theoretical predictions of the energy density formalism used with the sudden approximation.^{11,12} Results of full EFR-DWBA calculations for the one-nucleon stripping reaction, using deeper volume Woods-Saxon potentials with or without equal geometry for the real and imaginary parts, will be also presented later on in the section discussing the absolute cross section values; see Tables V

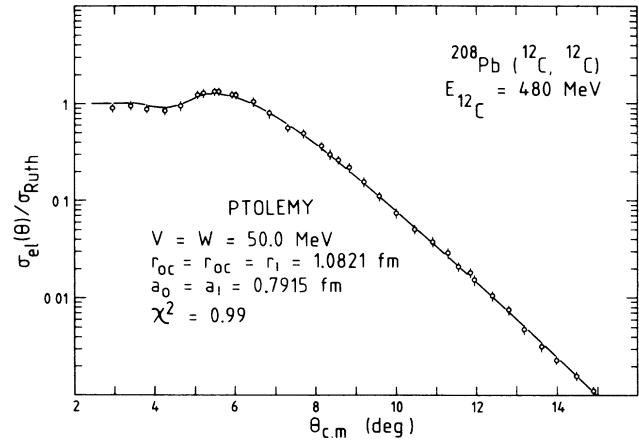


FIG. 3. Elastic scattering angular distribution of the 480 MeV ^{12}C beam on the ^{208}Pb target along with the optical model parameters of volume Woods-Saxon family $B3$ and the average chi-square value per point.

and VI of Sec. III C.

Figure 4 presents the results of the full EFR-DWBA calculations using the optical model parameter family of Fig. 3 which best fit the elastic scattering data, and using also the form factor parameters for the projectile and the heavy residual nucleus coming from Table III of Ref. 2. The spectroscopic factors were extracted using the usual formula:

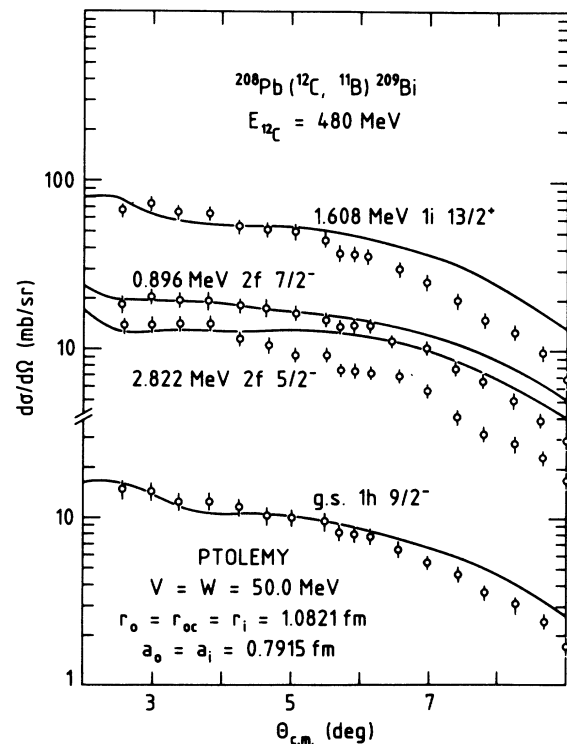


FIG. 4. Angular distributions for the $^{208}\text{Pb}(^{12}\text{C}, ^{11}\text{B})^{209}\text{Bi}$ one-proton stripping reaction. The solid lines are the results of EFR-DWBA calculations; see text and the spectroscopic factors of Table I.

TABLE I. One-proton spectroscopic factors for the ^{209}Bi final nucleus.

State	E^* (MeV)	($^{16}\text{O}, ^{15}\text{N}$) 793 MeV	($^{12}\text{C}, ^{11}\text{B}$) 480 MeV	(α, t) 80 MeV	Theory ^a
$1h_{\frac{9}{2}}^{-}$	g.s.	0.75	0.48	0.75	0.95
$2f_{\frac{7}{2}}^{-}$	0.896	0.67	0.66	0.71	0.85
$1i_{\frac{13}{2}}^{+}$	1.608	<u>0.70</u>	<u>0.70</u>	<u>0.70</u>	<u>0.70</u>
$2f_{\frac{5}{2}}^{-}$	2.822	0.74	0.80 ^b	0.54	0.66

^aAll the spectroscopic factors are normalized to the 1.608 MeV $1i_{\frac{13}{2}}^{+}$ state theoretical value, Ref. 15, this letter value is underlined in the table. The 1.608 MeV $1i_{\frac{13}{2}}^{+}$ level is the most strongly populated state in the ($^{12}\text{C}, ^{11}\text{B}$) reaction.

^bThe contribution of the 2.601 MeV $1i_{\frac{13}{2}}^{+}$ level has been subtracted assuming a spectroscopic factor of 0.06 for this state, Ref. 14.

$$d\sigma_{\text{expt}}(\theta) = NS_i S_f d\sigma_{\text{DWBA}}(\theta), \quad (1)$$

where S_i is the one-nucleon spectroscopic factor of the projectile-ejectile system and equals to 4 for ^{12}C nucleus: $1p_{\frac{3}{2}}^{-}$ orbit completely filled; S_f is the spectroscopic factor for the heavy residual nucleus; the cross section $d\sigma_{\text{DWBA}}(\theta)$ is provided by the code PTOLEMY (Ref. 9) and N is an overall normalization factor which is equal to 1 if the EFR-DWBA model is perfectly suitable to analyze such a direct stripping reaction assuming a one-step process. As a matter of fact, we can say that final state spectroscopic factors are known only in relative value. At the end of this paper we shall discuss the problem of normalization factor N whose value depends on the form factor parameters and on the optical model parameters.

It is worthwhile to note that the present geometry of the form factor parameters best fits the single particle state energies either of ^{209}Pb or ^{209}Bi see Ref. 3. It has also been checked that the code SATURN-MARS-I (Ref. 13) provided identical results as the code PTOLEMY (Ref. 9).

In Table I are presented the spectroscopic factors for the first single particle states of ^{209}Bi . In Fig. 1 it can be noticed that the $2f_{\frac{5}{2}}^{-}$ line located at 2.822 MeV excitation energy is broad. This is due to a contribution from the 2.601 MeV $1i_{\frac{13}{2}}^{+}$ state favored by the two selection rules. The spectroscopic factor of this $1i_{\frac{13}{2}}^{+}$ state is 0.06 (Ref. 14). In order to extract the spectroscopic factor of the $2f_{\frac{5}{2}}^{-}$ state, this small contribution was theoretically calculated and then subtracted. These spectroscopic factors are similar to those obtained previously in the ($^{16}\text{O}, ^{15}\text{N}$) reaction and in the (α, t) reaction,¹⁷ both performed on ^{208}Pb target. For the ($^{12}\text{C}, ^{11}\text{B}$) reaction, the g.s. spectroscopic factor seems to be too weak. In Table I we have quoted the results of a quasiparticle calculation¹⁵ which agree rather well with our results. Thus it can be concluded that EFR-DWBA calculations reproduce fairly well the relative intensities of the $^{208}\text{Pb}(^{12}\text{C}, ^{11}\text{B})^{209}\text{Bi}$ one-proton stripping reaction. However, the EFR-DWBA fits of Fig. 4 are rather poor at backward angles, inducing an uncertainty of about 10 to 20 % on the spectroscopic factor values.

Figure 5 presents the results of the EFR-DWBA calculations for the angular distributions of the

$^{208}\text{Pb}(^{12}\text{C}, ^{11}\text{C})^{209}\text{Pb}$ one-neutron stripping reactions measured at 480 MeV ^{12}C incident energy. As discussed previously, the form factor parameters come from Table III of Ref. 2 and best fit the single particle state excitation energies. The optical model parameters are those inset in Fig. 3, family B3, which best fit the ^{12}C elastic scattering data. The agreement between the experimental points and the calculated angular distributions is strikingly good for this one-neutron stripping reaction. Table II gives the spectroscopic factors extracted from this analysis. They

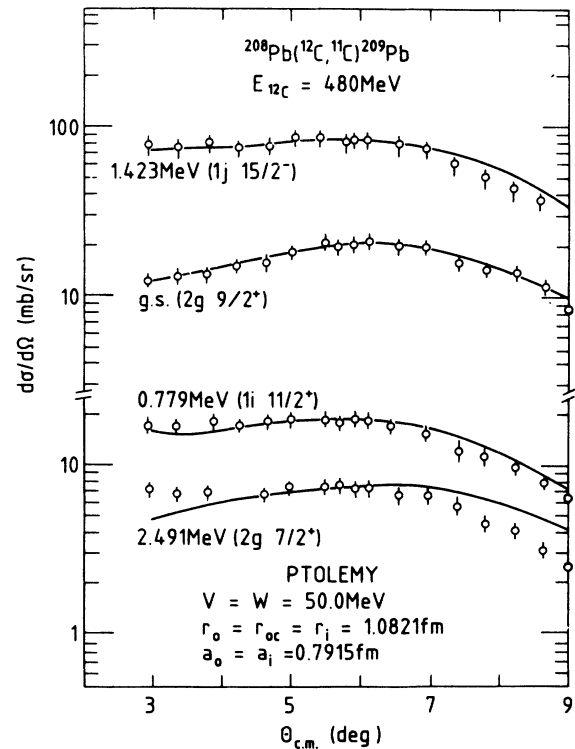


FIG. 5. Angular distributions for the $^{208}\text{Pb}(^{12}\text{C}, ^{11}\text{C})^{209}\text{Pb}$ one-neutron stripping reaction. The solid lines are the results of the EFR-DWBA calculations; see text and spectroscopic factors of Table II.

TABLE II. One-neutron spectroscopic factors for the ^{209}Pb final nucleus.

State	E^* (MeV)	($^{16}\text{O}, ^{15}\text{O}$) 793 MeV	($^{12}\text{C}, ^{11}\text{C}$) 480 MeV	($\alpha, ^3\text{He}$) 183 MeV	Theory ^a
$2g_{\frac{7}{2}}^+$	g.s.	0.89	0.80	0.76	0.89
$1i_{\frac{11}{2}}^+$	0.779	0.72	0.50	1.03	0.96
$1j_{\frac{15}{2}}^-$	1.423	<u>0.62</u>	<u>0.62</u> ^b	<u>0.62</u>	<u>0.62</u>
$2g_{\frac{7}{2}}^+$	2.491	0.79	0.92 ^c	0.98	0.84

^aAll spectroscopic factors are normalized to the 1.423 MeV $1j_{\frac{15}{2}}^-$ state theoretical value, Ref. 15, this latter value is underlined in the table. The 1.423 MeV $1j_{\frac{15}{2}}^-$ level is the most strongly populated state in the ($^{12}\text{C}, ^{11}\text{C}$) reaction.

^bFor the 1.423 MeV $1j_{\frac{15}{2}}^-$, it has been checked that the EFR-DWBA cross section of the unresolved 1.567 MeV $3d_{\frac{5}{2}}^+$ state is negligible due to the large momentum mismatch.

^cFor the $2g_{\frac{7}{2}}^+$, it has been checked that the EFR-DWBA cross section of the unresolved 2.537 MeV $3d_{\frac{3}{2}}^+$ state is negligible due to the large momentum mismatch and to the violation of the no spin-flip selection rule.

agree rather well with the previous data of the ($^{16}\text{O}, ^{15}\text{O}$) reaction and also with the quasiparticle calculations,¹⁵ exception made for the 0.779 MeV $1i_{\frac{11}{2}}^+$ level. Other theoretical spectroscopic factors of single particle states either for neutron or proton direct transfer reactions can be found in the review article of Mahaux *et al.*¹⁶ and references therein.

B. One-nucleon stripping reactions populating the higher excited states

Now we shall present a tentative analysis of the stripping reactions populating the higher excited levels of the ^{209}Bi and ^{209}Pb residual nuclei. For these levels the spin assignment is rather hypothetical and comes from Refs. 17 and 18. The main interest of these heavy ion reactions at high incident energy is that they populate strongly only high spin states. On the other hand our energy resolution is only 200 keV FWHM. Several excited levels can be seen in the spectrum of ^{209}Pb (Fig. 6): possible $1j_{\frac{15}{2}}^-$ and $1k_{\frac{17}{2}}^+$ candidates from the work of Massolo *et al.*¹⁸ Such levels of $l=7$ and $l=8$, respectively, are strongly favored by the two previous selection rules in the ($^{12}\text{C}, ^{11}\text{C}$) reaction. These levels can be followed at all the angles. They are the 3.02 MeV $1j_{\frac{15}{2}}^-$ level, the 3.59 MeV $1j_{\frac{15}{2}}^-$ and 3.73 MeV $1j_{\frac{15}{2}}^-$ doublet, and the 3.96 MeV $1k_{\frac{17}{2}}^+$ and 4.22 MeV $1k_{\frac{17}{2}}^+$ doublet. Above this group of levels, broad structures can be observed on the various energy spectra around an excitation energy of 10 MeV which is the energy position of giant quadrupole resonance, see Ref. 19.

Figure 7 presents the angular distribution of the excited levels of ^{209}Pb heavy residual nucleus. The values of the experimental points were obtained by a best fit procedure of the energy spectrum lines without any background. The agreement in shape of the angular distribution is rather reasonable. The corresponding spectroscopic factors are listed in Table III. They agree more or less with the ones obtained by the ($\alpha, ^3\text{He}$) experiment,¹⁸ exception made of the hypothetical $1k_{\frac{17}{2}}^+$ doublet located at 4.1 MeV excitation energy. This doublet is un-

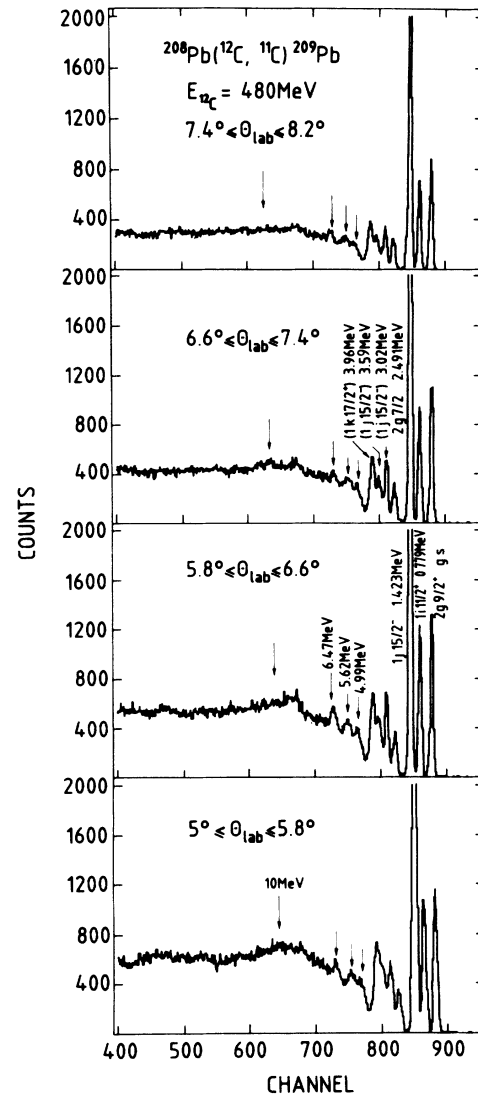


FIG. 6. Energy spectra of the $^{208}\text{Pb}(^{12}\text{C}, ^{11}\text{C})^{209}\text{Pb}$ one-neutron stripping reaction at several laboratory angles presented in order to follow the weakly excited states of high spin located at high excitation energies.

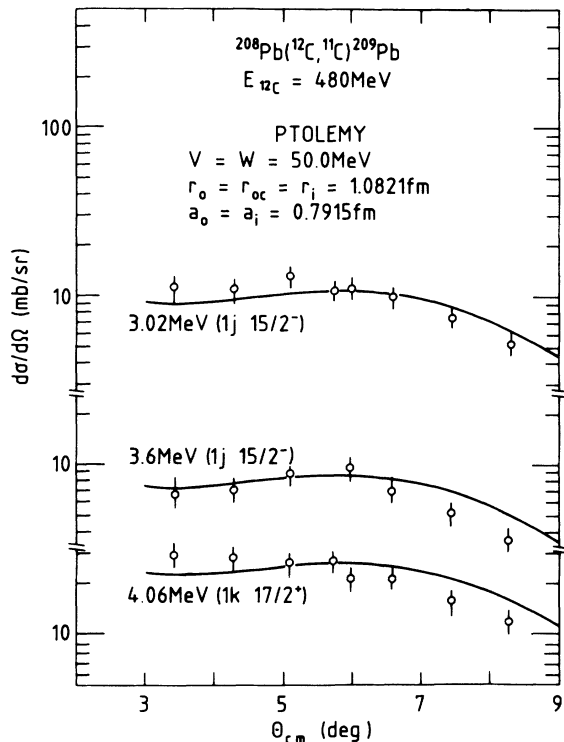


FIG. 7. Angular distributions for the $^{208}\text{Pb}(^{12}\text{C}, ^{11}\text{C})^{209}\text{Pb}$ one-neutron stripping reaction. The solid lines are the results of the EFR-DWBA calculations. See text and spectroscopic factors of Table III.

bound and the EFR-DWBA analysis has been performed in the following way. First of all, the experimental Q value is input in the PTOLEMY (Ref. 9) code for the distorted wave calculations: the usual procedure. However, the $1k_{\frac{17}{2}}^{+}$ wave function is arbitrarily bound by -0.10 MeV. It has been checked that a binding energy of -0.50 MeV increases the spectroscopic factor values by only 8%. It is worthwhile to note that the $1k_{\frac{17}{2}}^{+}$ doublet excitation energy is very near to the ^{209}Pb neutron binding energy: 3.9364 MeV. So we may have some

TABLE III. One-neutron spectroscopic factors or sums for the ^{209}Pb final nucleus. All spectroscopic factors of ^{209}Pb are normalized on the 1.423 MeV $1j_{\frac{15}{2}}^{-}$ theoretical value of Table II; the spin assignments between parentheses are rather hypothetical and come from Ref. 18.

State	E^* (MeV)	$(^{12}\text{C}, ^{11}\text{C})$ 480 MeV	$(\alpha, ^3\text{He})$ 183 MeV
$1j_{\frac{15}{2}}^{-}$	3.02	0.085	0.057
$(1j_{\frac{15}{2}}^{-})$	3.59		
		0.065	0.076
$(1j_{\frac{15}{2}}^{-})$	3.73		
$(1k_{\frac{17}{2}}^{+})$	3.96		
		0.13	0.064
$(1k_{\frac{17}{2}}^{+})$	4.22		

confidence about this procedure of spectroscopic-factor extraction. It is also worthwhile to note that Hartree-Fock calculations predict a $1k_{\frac{17}{2}}^{+}$ level around 6 MeV excitation energy.⁸

Figure 8 presents the one-proton stripping reaction spectra measured at several angles. Several states at higher excitation energy can be followed at each angle between the 3.87 MeV $1i_{\frac{13}{2}}^{+}$ state and the 5.44 MeV $1j_{\frac{15}{2}}^{-}$, $1i_{\frac{11}{2}}^{+}$ unresolved multiplet. Furthermore, as in the one-

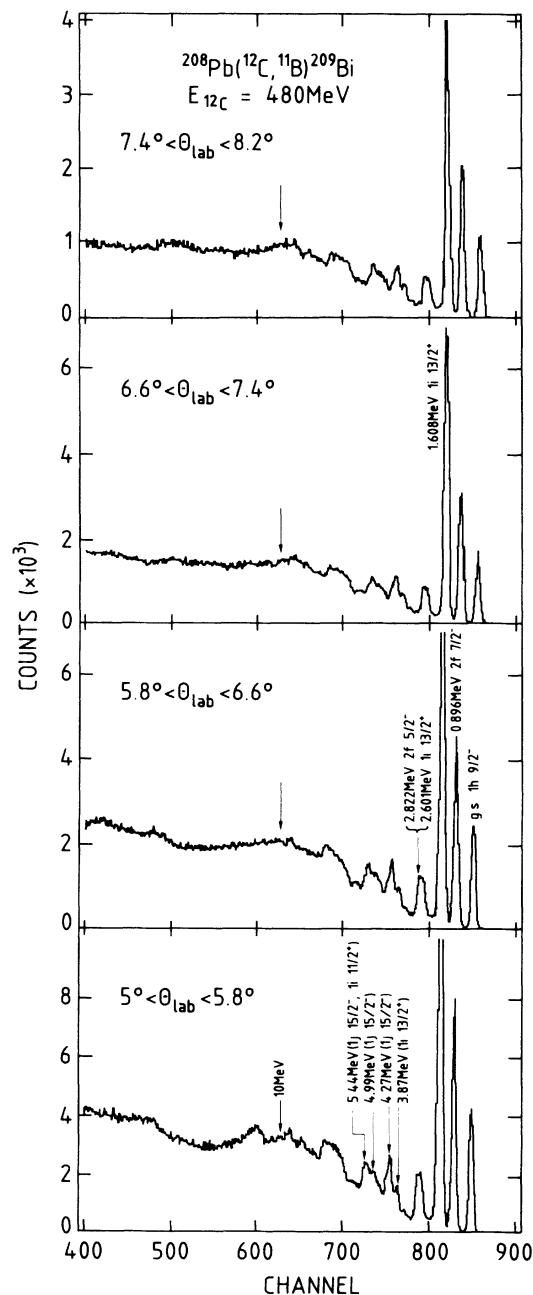


FIG. 8. Energy spectra of the $^{208}\text{Pb}(^{12}\text{C}, ^{11}\text{B})^{209}\text{Bi}$ one-proton stripping reaction at several laboratory angles presented in order to follow the weakly excited states of high spins located at high excitation energies.

neutron stripping reaction, a structure at an excitation energy of about 10 MeV can be seen for which only speculation can be made about its origin: excitation in a two-step process of single-particle states coupled to the target giant quadrupole resonance. The cross-section values were extracted from these energy spectra using a best fit procedure with a smooth empirical background going through the deepest valley of the energy spectra. This procedure will give rise to a large uncertainty in the spectroscopic factor values. Figure 9 presents EFR-DWBA fits of the angular distributions of these excited levels which are all unbound, the proton binding energy is 3.7980 MeV, and in these calculations the wave functions have been arbitrarily bound by -0.10 MeV. Exception made of the 4.26 MeV $1j_{1/2}^{15-}$ state, the fits are rather acceptable and the corresponding spectroscopic factors or their sums are given in Table IV. The $1i_{1/2}^{13+}$ states and all the fragmented $1j_{1/2}^{15-}$ states are strongly favored by the two selection rules. On the other hand, the populations of the $1i_{1/2}^{11+}$ states are inhibited due to their spin flip transition. Exception made of the higher excited multiplet, the agreement of the spectroscopic factors between the ($^{12}\text{C}, ^{11}\text{B}$) and (α, t) experiments¹⁷ is almost satisfactory.

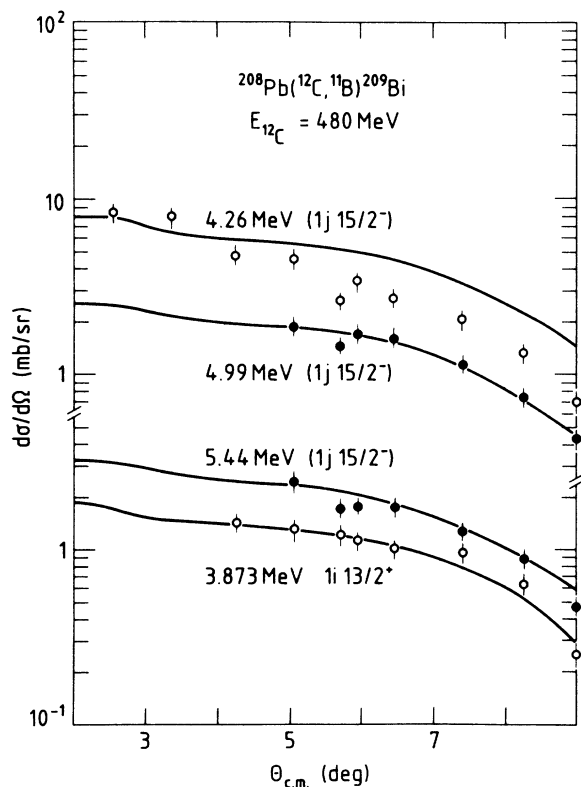


FIG. 9. Angular distribution for the $^{208}\text{Pb}(^{12}\text{C}, ^{11}\text{B})^{209}\text{Bi}$ one-proton stripping reaction. The solid lines are the results of the EFR-DWBA calculations; see text and spectroscopic factors of Table IV.

TABLE IV. One-proton spectroscopic factors or sums for the ^{209}Bi final nucleus. All spectroscopic factors of ^{209}Bi are normalized on the 1.608 MeV $1i_{1/2}^{13}$ theoretical value of Table I. The spin assignments between parentheses are rather hypothetical and come from Ref. 17.

State	E^* (MeV)	($^{12}\text{C}, ^{11}\text{B}$) 480 MeV	(α, t) 80 MeV
$1i_{1/2}^{13+}$	3.835	0.017	0.028
$(1j_{1/2}^{15-})$	4.17		
		0.063	0.099
$(1j_{1/2}^{15-})$	4.27		
$(1j_{1/2}^{15-})$	4.88		
		0.021	0.047
$(1j_{1/2}^{15-})$	4.99		
$(1j_{1/2}^{15-})$	5.27		
$(1j_{1/2}^{15-})$	5.38	0.018	0.16
$(1i_{1/2}^{11+})$	5.47		
$(1i_{1/2}^{11+})$	5.58		

C. The EFR-DWBA predictions of cross section absolute values

We are going to discuss now the problem of the absolute values for the cross sections at high incident energies. Although the EFR-DWBA calculations predict correctly the absolute cross-section values for the one-nucleon stripping reactions induced by the 480 MeV ^{12}C beam, it has turned out that for the one-nucleon stripping reactions induced by the 793 MeV ^{16}O beam the absolute cross-section values are overpredicted by a factor of 5–10, see Refs. 4 and 5.

In order to study the stability of the cross-section values with respect to the variation of the optical model parameters for the ^{12}C beam experiments, we have tried a deeper volume Woods-Saxon family of potentials, namely $V=W=200$ MeV, which also best fits the elastic scattering data. Thus potential is drawn in Fig. 10 along with the $V=W=50$ MeV family. We can see that both families exhibit the same tails. This fact is just the signature of the continuous Igo ambiguity.¹⁰ This new $V=W=200$ MeV family reproduces perfectly well the data and provides the stripping cross sections with almost the same absolute values; in other words, the same normalization coefficient N , see formula (1). These two families (the 50 MeV and 200 MeV), have equal geometry for the real and imaginary part. To check the sensibility to this feature we have also performed calculations with families having a different geometry for the real and imaginary part. They were obtained by increasing or decreasing the radius parameter of the imaginary part by 30%, 20%, or 10% and then searching with the automatic code PTOLEMY (Ref. 9) for the best elastic scattering fit by varying the imaginary depth and imaginary diffusivity and keeping the same real part geometry of the $V=200$ MeV or of the $V=50$ MeV family *A* and *B*, respectively. In Table V are listed the various potentials with their corresponding χ^2 values for elastic scattering and with the

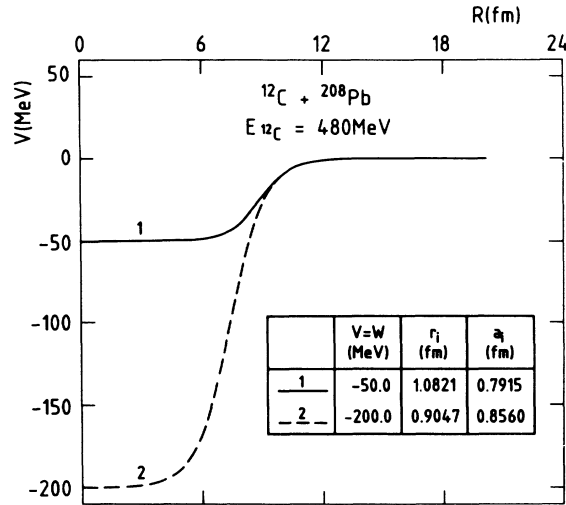


FIG. 10. Real and imaginary part of the volume Woods-Saxon family *A*3 and *B*3 used for the various EFR-DWBA calculations. Both potentials best fit the ^{12}C elastic scattering data on ^{208}Pb target.

normalization coefficient N values. These coefficients N were determined from the g.s. transitions using the corresponding experimental spectroscopic factors of ^{209}Bi and ^{209}Pb final nuclei, respectively, see Tables I and II. The imaginary parts of the various potentials are plotted in Figs. 11 and 12. The following comments can be made. All the optical potentials which have the same tails produce both excellent EFR-DWBA fits for the one-nucleon stripping angular distributions and reasonable normalization coefficients N . This is the case for all the families *A* (*A*1–*A*5) and for the families *B*3, *B*4, and *B*5. Families *B*1 and *B*2 are dubious, producing very poor EFR-DWBA fits for the one-nucleon stripping reaction, and, furthermore, their elastic scattering χ^2 values are not very good. From Fig. 12 we can see that their tails are not correct since their imaginary wells are not deep enough.

The same systematic analysis was also performed for the one-nucleon stripping reactions induced by the 793 MeV ^{16}O beam on a ^{208}Pb target. Figure 13 shows a typical result of an EFR-DWBA analysis obtained for the (^{16}O , ^{15}N) one-proton stripping reaction, with the $V=W=200$ MeV family *C*3. The agreement in shape for the angular distributions is strikingly good and the corresponding spectroscopic factors are similar to those quoted in Table I. Let us also note that the (^{16}O , ^{15}O) one neutron stripping reaction on ^{208}Pb provides similar spectroscopic factors as those of (^{12}C , ^{11}C) reaction, see Ref. 5. Table VI presents for the one-neutron and the one proton stripping reactions the normalization coefficients N of the EFR-DWBA analyses performed with potentials similar to those used for the ^{12}C beam and listed already in Table V. As previously, these coefficients N are determined from the g.s. transitions using the corresponding spectroscopic factors of Ref. 5 for ^{209}Bi and ^{209}Pb final nuclei. All the *C* families (200 MeV deep potential for the real part) produce similar EFR-DWBA fits for the transfer data and a similar coefficient of normalization N of the order of 0.15. The same results are reached for the families *D*3, *D*4, and *D*5, having a real potential 50 MeV deep. Nevertheless, for the shallow imaginary well, families *D*1 and *D*2 fail to reproduce the experimental data in shape and in absolute value.

All the EFR-DWBA curves obtained with the optical model parameters which reproduce the entrance channel elastic scattering are very similar and produce normalization factors obtained in the same consistent way. However, the DWBA fits are not very good in case of (^{12}C , ^{11}B) one proton stripping reactions exception mode of the g.s. transition. It is generally considered that spectroscopic factors and normalization coefficients have to be extracted by fitting the experimental angular distributions at forward angles where the theoretical curves are less dependent of the optical model parameters. Normalization factors taking more into account the backward angle measurements will decrease the normalization factor by 20% especially for the excited levels of ^{209}Bi . It has been shown by Peng *et al.*, Ref. 20, that in case of Fresnel elastic scattering pattern in the entrance and exit channels,

TABLE V. Coefficient N of normalization for the one-nucleon stripping reactions for the system $^{12}\text{C}+^{208}\text{Pb}$ at 480 MeV incident energy. Real part of the volume Woods-Saxon families *A*: $V=200.0$ MeV, $r_0=r_{0c}=0.9047$ fm, $a=0.8360$ fm. Real part of the volume Woods-Saxon families *B*: $V=50.0$ MeV, $r_0=r_{0c}=1.0821$ fm, $a=0.7915$ fm.

Family	W (MeV)	r_i (fm)	a_i (fm)	χ^2	$N(^{12}\text{C}, ^{11}\text{B})$	$N(^{12}\text{C}, ^{11}\text{C})$
<i>A</i> 1	25.	1.176	0.812	1.93	0.97	1.11
<i>A</i> 2	42.4	1.085	0.819	1.12	0.64	0.83
<i>A</i> 3	200.	0.904	0.856	1.16	0.74	0.87
<i>A</i> 4	473.	0.814	0.850	1.29	0.73	0.85
<i>A</i> 5	1111.4	0.723	0.853	1.25	0.74	0.86
<i>B</i> 1	8.2	1.406	0.574	5.02	0.28	1.32
<i>B</i> 2	10.2	1.298	0.658	1.53	0.24	0.74
<i>B</i> 3	50.	1.082	0.791	0.99	0.79	0.98
<i>B</i> 4	134.2	0.973	0.811	1.16	0.83	0.94
<i>B</i> 5	378.8	0.865	0.822	1.29	0.92	1.00

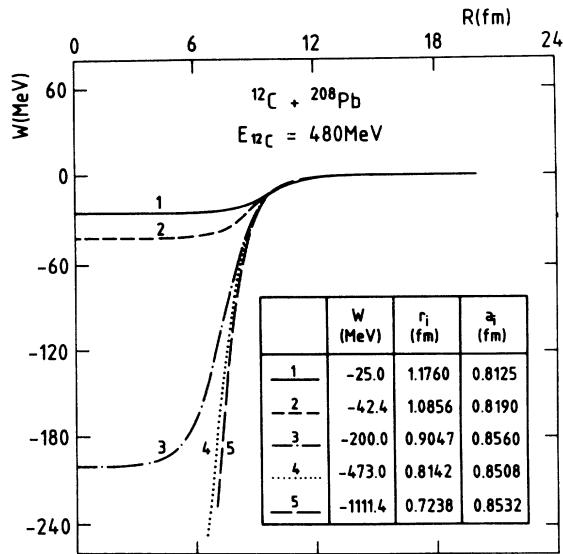


FIG. 11. Volume Woods-Saxon imaginary part of the optical model potential used in the EFR-DWBA calculations. The real parts of all these families have their parameters equal to those of family A3. All best fit the elastic scattering data. It has turned out that all these potentials produce the same results for the elastic scattering cross sections and for the one-nucleon stripping cross sections since they have the very same tails.

the optical model parameters can be very alike for both channels; see Figs. 3 and 4 of Ref. 21. Due to this fact and in order to avoid any arbitrariness, we have not tried to improve the EFR-DWBA fits in case of ($^{12}\text{C}, ^{11}\text{B}$) one proton stripping reactions, by using different optical model parameters for the entrance and exit channels.

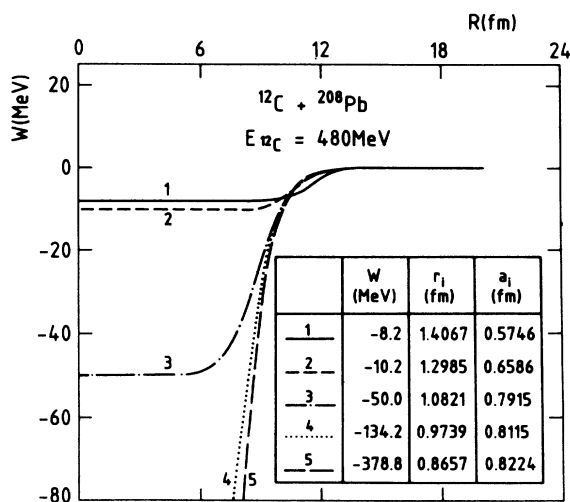


FIG. 12. Volume Woods-Saxon imaginary part of the optical potential used in the EFR-DWBA calculations. Families B1 and B2 do not reproduce successfully the elastic scattering data and the transfer data, while the other families do.

The normalization coefficients, N , can be slightly decreased by increasing the radii of the form factor. For the bound state wave function of the heavy residual partners the radius parameters are already large 1.28 and 1.25 fm for the ^{209}Bi and ^{209}Pb , respectively, but for the ^{12}C projectile an increase of the radius parameter from 1.20 fm to 1.25 fm produces a decrease of the normalization coefficient of 10%. Furthermore, the value of the normalization coefficient N , depends, according to formula (1), on the value of the entrance channel spectroscopic factor. We have taken so far crude shell model estimates: 4 and 2, respectively, for the ^{12}C and ^{16}O projectiles. However, from the $^{12}\text{C}(^3\text{He}, \alpha)^{11}\text{C}$ pick-up reaction and $^{12}\text{C}(p, d)^{11}\text{C}$ pick-up reaction the spectroscopic factors are 3.06 and 2.5, respectively.²¹ These values will increase the normalization coefficient N by 24% and 38%, respectively. For the ^{16}O projectile, we are dealing with a double magic nuclei. Thus a value of 2 for the probably completely filled $1p_{1/2}$ subshell is a very reasonable assumption which is confirmed by the experimental spectroscopic factor values extracted from the one nucleon pick-up reactions induced by deuteron beam on ^{16}O target nucleus, see Ref. 22.

To summarize the results about one-nucleon stripping reactions induced either by a ^{12}C beam or a ^{16}O beam, we

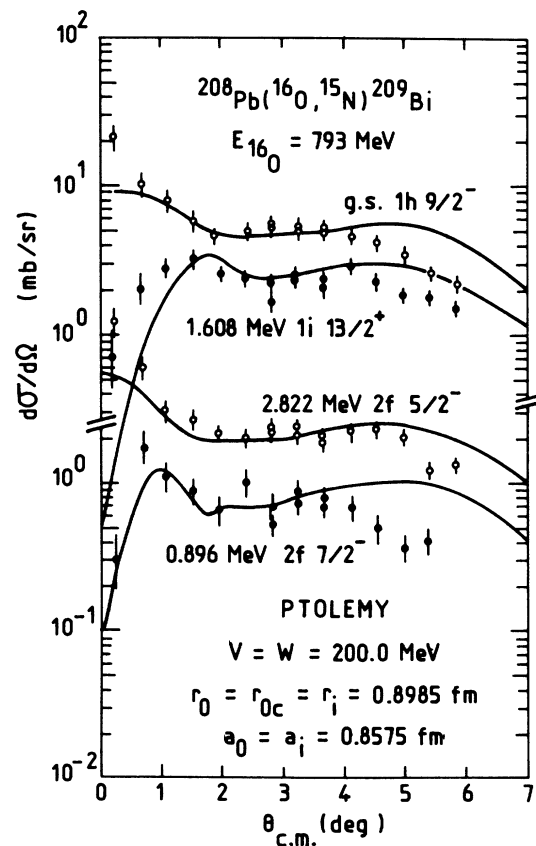


FIG. 13. Angular distributions for the $^{208}\text{Pb}(^{16}\text{O}, ^{15}\text{N})^{209}\text{Bi}$ one-proton stripping reaction. The solid lines are the results of the EFR-DWBA calculation; see text. The corresponding normalization coefficient, N , is given in Table VI, family C3.

TABLE VI. Same as Table V for the system $^{16}\text{O}+^{208}\text{Pb}$ at 793 MeV incident energy. Real part of the volume Woods-Saxon families C: $V=200.0$ MeV, $r_0=r_{0c}=0.8983$ fm, $a=0.8575$ fm. Real part of the volume Woods-Saxon families D: $V=50.0$ MeV, $r_0=r_{0c}=1.0970$ fm, $a=0.7260$ fm.

Family	W (MeV)	r_i (fm)	a_i (fm)	χ^2	$N(^{16}\text{O}, ^{15}\text{N})$	$N(^{16}\text{O}, ^{15}\text{O})$
C1	24.9	1.168	0.775	3.04	0.17	0.15
C2	42.3	1.078	0.805	2.04	0.13	0.11
C3	200.0	0.898	0.857	1.65	0.14	0.15
C4	454.4	0.808	0.844	1.60	0.12	0.11
C5	1023.9	0.718	0.853	1.62	0.12	0.11
D1	5.10	1.426	0.253	2.67	0.01	0.03
D2	8.98	1.316	0.602	3.98	0.03	0.11
D3	50.0	1.096	0.726	1.70	0.18	0.17
D4	113.6	0.987	0.748	1.61	0.12	0.10
D5	358.6	0.877	0.761	1.60	0.13	0.11

can say that the normalization coefficients are of the order of 1 for the 480 MeV ^{12}C projectile and of the order of 0.10–0.20 for the 793 MeV ^{16}O projectile. Let us note that the normalization coefficient was already 0.35 at 312 MeV ^{16}O incident energy for this latter projectile, see Ref. 2. On the other hand, one neutron pick-up reactions and one neutron stripping reactions induced by several ^{12}C beams in the vicinity of the Coulomb barrier on ^{208}Pb target have provided EFR-DWBA normalization factors N of the order of unity, see Ref. 23.

This difference does not come from the theoretical calculations but is a true experimental fact. For instance, in the one nucleon stripping reaction induced by a ^{16}O projectile, the highest cross sections are 5.5 mb/sr for the $1h_{\frac{9}{2}}^-$ g.s. of ^{209}Bi and 6 mb/sr for the $1i_{\frac{11}{2}}^+$ state of ^{209}Pb at the same 4.2° c.m. angle, respectively, while in case of ^{12}C projectile the highest cross sections are 55 mb/sr for the $1i_{\frac{13}{2}}^+$ state of ^{209}Bi and 72 mb/sr for the $1j_{\frac{15}{2}}$ state of ^{209}Pb : basically a factor of 10 in the experimental cross section values for the two different projectiles. Thus one proton and one neutron stripping reactions appear to be inhibited at high incident energy for ^{16}O beams.

These results about the ^{16}O beams are rather puzzling since for the one proton pick-up and one-neutron stripping reactions induced by the ^{18}O projectile bombarding a ^{28}Si target at 352 MeV incident energy the normalization factors are also equal to unity for strong absorption potential.²⁴ Furthermore, single-nucleon transfer reactions induced by 376 MeV ^{17}O beam on a ^{208}Pb target²⁵

and by ^{28}Si beams of 6 and 8 MeV/nucleon incident energy, respectively, are also correctly predicted by EFR-DWBA calculations.²⁶

IV. CONCLUSION

At very high incident energy it has turned out that the relative intensities for the population of single-particle states are governed by two selection rules contained either in the EFR-DWBA or in the semiclassical model. The strongest excited levels are single-particle high-spin states populated without spin flip. Reliable spectroscopic factors can be extracted at high incident energy as well as at low energy. Absolute values of cross sections are correctly predicted by the EFR-DWBA using strong absorption optical model potentials, where both elastic scattering cross sections and transfer reaction data are well fitted. However, in the case of ^{16}O beam the EFR-DWBA calculations fail completely to reproduce the cross sections in terms of absolute values; and this is a rather puzzling problem.

ACKNOWLEDGMENTS

It is a pleasure to thank Professor C. A. Whitten, Jr. from the University of California, Los Angeles for careful reading of the manuscript and enlightening discussions. Sincere thanks are also due to Mrs. J. Sauret and the operating staff of the GANIL cyclotrons for the excellent quality of the 480 MeV ^{12}C beam.

¹T. Tamura, T. Udagawa, and M. C. Mermaz, Phys. Rep. **65**, 346 (1980); and N. K. Glendenning, Rev. Mod. Phys. **47**, 659 (1975).

²C. Olmer, M. C. Mermaz, M. Buenerd, C. K. Gelbke, D. L. Hendrie, J. Mahoney, D. K. Scott, M. H. Macfarlane, and S. C. Pieper, Phys. Rev. C **18**, 205 (1978).

³S. C. Pieper, M. H. Macfarlane, D. H. Gloeckner, D. G. Kovar, F. D. Becchetti, B. G. Harvey, D. L. Hendrie, H. Homeyer, J. Mahoney, F. Pühlhofer, W. von Oertzen, and M.

S. Zisman, Phys. Rev. C **18**, 180 (1978).

⁴B. Berthier, J. Barrette, J. Gastebois, A. Gillibert, R. Lucas, J. Matuszek, M. C. Mermaz, A. Miczaika, E. van Renterghem, T. Suomijärvi, A. Boucenna, D. Disdier, P. Gorodetzky, L. Kraus, I. Linck, B. Lott, V. Rauch, R. Rebmeister, F. Scheibling, N. Schulz, J. C. Sens, C. Grunberg, and W. Mittag, Phys. Lett. **B182**, 15 (1986).

⁵M. C. Mermaz, B. Berthier, J. Barrette, J. Gastebois, A. Gillibert, R. Lucas, J. Matuszek, A. Miczaika, E. Van Renter-

- ghem, T. Suomijärvi, A. Boucenna, D. Disdier, P. Gorodetzky, L. Kraus, I. Linck, B. Lott, V. Rauch, R. Rebmeister, F. Scheibling, N. Schultz, J. C. Sens, C. Grunberg, and W. Mittag, *Zeit. Phys.* **A326**, 353 (1987).
- ⁶D. M. Brink, *Phys. Lett.* **40B**, 37 (1972).
- ⁷F. Pougheon, P. Roussel, P. Colombani, A. Doubre, and J. Roynette, *Nucl. Phys.* **A193**, 305 (1972); F. Pougheon and P. Roussel, *Phys. Rev. Lett.* **30**, 1223 (1973); P. Roussel, *J. Phys. (Paris) Colloq.* **41**, C3-129, (1980); and W. von Oertzen, *Phys. Lett.* **151B**, 95 (1985).
- ⁸P. Birien and S. Valéro, Report CEA-N-2215 CEN Saclay, France, (1981); and J. Gastebois, *Lecture Notes in Physics* (Springer, Berlin, 1983), Vol. 178, p. 126.
- ⁹M. H. Macfarlane and S. C. Pieper, Argonne National Laboratory, Report ANL-76-11, 1976.
- ¹⁰G. Igo and R. M. Thaler, *Phys. Rev.* **106**, 126 (1957).
- ¹¹H. Ngô and Ch. Ngô, *Nucl. Phys.* **A348**, 140 (1980).
- ¹²A. Faessler, R. Linden, N. Ohtsuka, and F. B. Malik, *J. Phys. (Paris) Colloq.* **47**, C4-111c (1986).
- ¹³T. Tamura and K. S. Low, *Comput. Phys. Commun.* **8**, 349 (1974).
- ¹⁴C. Ellegaard and P. Vedelsby, *Phys. Lett.* **26B**, 155 (1968).
- ¹⁵P. Ring and E. Werner, *Nucl. Phys.* **A211**, 198 (1973).
- ¹⁶C. Mahaux, P. F. Bortignon, R. A. Broglia, and C. H. Dasso, *Phys. Rep.* **120**, 1 (1985).
- ¹⁷S. Gales, C. P. Massolo, S. Fortier, J. P. Shapira, P. Martin, and V. Comparat, *Phys. Rev. C* **31**, 94 (1985).
- ¹⁸C. P. Massolo, F. Azaiez, S. Gales, S. Fortier, E. Gerlic, J. Guillet, E. Hourani, and J. M. Maison, *Phys. Rev. C* **34**, 1256 (1986).
- ¹⁹Ph. Chomaz, *J. Phys. (Paris) Colloq.* **47**, C4-155 (1986).
- ²⁰J. C. Peng, B. T. Kim, M. C. Mermaz, A. Greiner, and N. Lisbona, *Phys. Rev. C* **18**, 2179 (1978).
- ²¹F. Ajzenberg-Selove and C. Langell-Busch, *Nucl. Phys.* **A336**, 41 (1980).
- ²²K. H. Purser, W. P. Alford, D. Cline, H. W. Fulbright, H. E. Gove, and M. S. Krick, *Nucl. Phys.* **A132**, 75 (1969); and F. Ajzenberg-Selove, *ibid.* **A360**, 140 (1981).
- ²³K. S. Toth, J. L. C. Ford, Jr. G. R. Satchler, E. E. Gross, D. C. Hensley, S. T. Thornton, and T. C. Schneizer, *Phys. Rev. C* **14**, 1471 (1976).
- ²⁴M. A. G. Fernandes, B. L. Burks, D. J. Horen, G. R. Satchler, R. L. Auble, F. E. Bertrand, J. L. Blankenship, J. L. C. Ford, Jr., E. E. Gross, D. C. Hensley, R. O. Sayer, D. Shapira, and T. P. Sjoreen, *Phys. Rev. C* **33**, 1971 (1986).
- ²⁵M. A. G. Fernandes, F. E. Bertrand, R. L. Auble, R. O. Sayer, B. L. Burks, D. J. Horen, E. E. Gross, J. C. Blankenship, D. Shapira, and M. Beckerman, *Phys. Rev. C* **36**, 108 (1987).
- ²⁶J. J. Kolata, K. E. Rehm, D. G. Kovar, G. S. F. Stephans, G. Rosner, H. Ikezoe, and R. J. Vojtech, *Phys. Rev. C* **30**, 125 (1984); and J. J. Kolata, L. A. Lewandowski, K. E. Rehm, D. G. Kovar, G. S. F. Stephans, G. Rosner, H. Ikezoe, and M. F. Vineyard, *ibid.* **35**, 2139 (1987).